JOURNAL OF MATERIALS SCIENCE 29 (1994) 2981–2986

Amorphous phase growth by isothermal annealing-induced interdiffusion reactions in mechanically deformed Ni/Ti multilayered composites

T. D. SHEN*, M. X. QUAN, J. T. WANG, Z. Q. HU
*State Key Lab of RSA, Institute of Metal Research, *and also International Centre for Materials Physics, Academia Sinica, Wenhua Road 72, Shenyang 110015, People's Republic of China*

The growth of amorphous phase and the formation of competing intermetallic compounds in mechanically deformed Ni/Ti multilayered composites have been investigated by X-ray diffraction, scanning electron microscopy, transmission electron micrography, and magnetic measurement. Experimental observations in the Ni/Ti system have been performed, supporting a transient nucleation model for solid-state amorphization. The amorphous layers in the Ni/Ti multilayered composites continue to grow until they have attained a temperature-dependent critical thickness or a temperature-dependent critical annealing time. The relationships between the critical amorphous layer thickness and temperature, between the critical annealing time and temperature, and between the annealing conditions (temperature, time) and amorphization transformation, have been deduced and compared with the experimental results. The quantitative relationships can give a direction for the bulk amorphization in the Ni/Ti multilayered composites.

1. Introduction

The recent discovery [1–4] of amorphous-phase formation by solid-state reaction of layered crystalline material has generated interest in the fundamental nature of this process, as well as excitement over its application for formation of bulk amorphous materials [3, 5–14]. Since the first reports of amorphization during isothermal annealing of metal–metal multilayers by solid-state reaction [1], many binary systems, e.g. La–Au [1], Ni–Zr [3, 5, 7, 9, 14], Ni–Er [6], Cu–Er [6], Cu–Zr [8], Co–Zr [10], Ni–Ti [9, 11], have been amorphized by this technique. One of the methods to prepare metal multilayers is mechanical deformation [3, 5], with which it is possible by the solid-state amorphization reaction (SSAR) in a multilayer composite to produce bulk amorphous alloys of basically any shape and size if one can prepare a very fine composite of the two crystalline components. However, the kinetics of the SSAR in the multilayer composite has not been clearly known. For example, although the equilibrium phase diagram and thermodynamic condition of the Ni/Ti and Ni/Zr systems are similar, the amorphous phase has been observed to grow to a thickness of up to 100 nm at Ni/Zr interfaces [15–17]; such prodigious growth has not been observed in the Ni/Ti multilayer composites [18–20]. Bulk amorphization in the Ni/Ti system has not been obtained so far, which was thought to be the result of too thick elemental layers, of an annealing treatment not yet optimized, or of thermodynamic conditions [11].

It was found that all multilayer diffusion couples in which significant fractions of amorphous phases formed upon annealing had the common properties of a large negative heat of mixing, ΔH_{mix}, and a large asymmetry of atomic diffusivities of the two constituent species or $D_B \gg D_A$ [1, 21]. However, few quantitative studies of the amorphization process in the metal multilayer systems have been made. In particular, the dependencies of thermodynamic and kinetic parameters, of annealing treatment conditions, e.g. temperature and time, and of single-layer thickness of the original A–B multilayer on the amorphous phase growth, require more data and discussion. In our previous paper [22] we studied the microstructures, the SSAR induced by a constant heating-rate annealing, and the corresponding kinetic data for the mechanically deformed Ni/Ti multilayered composites. In the present work we investigated the SSAR quantitatively in the mechanically deformed Ni/Ti multilayers having undertaken an isothermal anneal.

2. Experimental procedure

$Ni_{65}Ti_{35}$ (at %) composite powders (99.5%, 50–70 μm), in which a titanium core with a thickness of 30–50 μm was coated by a thin layer of nickel with a thickness of 5–10 μm [23], was used as starting materials. The $Ni_{65}Ti_{35}$ composite powders were prepared by a chemical method, during which the composition could be controlled accurately. Ni/Ti multilayer was prepared by consolidating the composite

0022–2461

powders, sealing them in a steel can and subsequently cold rolling the sample plus can. The sample obtained was then removed from the can and subsequently cold rolled in ten passes, each consisting of an overlap of several (two to four) pieces of sample to increase its thickness and rolling it to the thickness, 0.8 mm, of the minimum spacing of the rollers. The oxygen content of $Ni_{65}Ti_{35}$ composites before and after cold rolling was 0.17 and 0.26 wt %, respectively, as measured by a KLS-56 coulomb analytical instrument.

Samples which were to be thermally reacted were vacuum sealed with zirconium getters ($Zr_{84}Al_{16}$, weight ratio) in long Pyrex tubes. Prior to sample annealing, the getters were separately heated to 500 °C for 10 h while the samples remained at ambient temperature.

The microstructure and amorphization of Ni/Ti multilayers were monitored by X-ray diffraction (XRD), scanning electron microscopy (SEM), transmission electron microscopy (TEM), and magnetic measurement. The XRD experiments were carried out in a Rigaku X-ray diffractometer using CuK_α radiation ($\lambda = 0.154$ nm). A Philips EM420 microscope equipped with EDAX detector operated in the standardless mode was used for the TEM experiment. For the preparation of TEM samples, the multilayer sample was mixed with epoxy, thin slices were cut along the direction of the surface of the sample with a hardened steel knife. The cut slices were suspended in anhydrous alcohol, a few drops of which were placed on to a carbon-supported film just prior to insertion into the transmission electron microscope. This method rules out the possibility of amorphization during the sample preparation process. The saturation magnetization at room temperature was measured by a vibrating sample magnetometer at a magnetic field of 760 kA m^{-1}.

3. Results

The microstructure of the mechanically deformed Ni/Ti multilayers has been reported [22]: the XRD profiles show that the initially sharp crystalline diffraction peaks are considerably broadened after several rolling passes as a result of the refinement of microcrystalline size and of the increase of internal strain. The rolled product consists of many Ni/Ti couples having an almost constant thickness, as seen from the optical micrograph (OM) and SEM techniques [22]. The average single-layer thickness, ASLT, for the Ni/Ti multilayered samples after 2, 8 and 10 passes of cold rolling, is about 1, 0.2 and 0.09 μm, respectively, as estimated from OM and SEM observation [22]. The multilayered sample after 10 passes of cold rolling is designated CR10.

The measured density of the rolled product after only one pass of cold rolling is 6.475 g cm^{-3}, which is approximately 94.4% of the theoretical density, 6.860 g cm^{-3}, of the $Ni_{65}Ti_{35}$ composite material. This indicates that the void percentage of the rolled samples is rather small.

The isothermal annealing conditions for the CR10 sample are shown in Table I. The XRD profiles for the as-deformed sample, CR10, and annealed samples are shown in Fig. 1. The amorphous phase has not been observed in the as-deformed CR10 sample within the resolution of the XRD technique. However, the Ni(1 1 1) Bragg peaks in the XRD patterns for the annealed samples (A1, B1 and C1) become very asymmetrical. This is attributed to the formation of an amorphous Ni–Ti alloy which results in an additional

TABLE I Isothermal annealing temperature, T, isothermal annealing time, t, experimentally chosen, and critical annealing time at temperature T, $t^*(T)$, theoretically calculated.

	A1	A2	B1	B2	C1	C2
t (h)	100	190	7	10	0.9	1.3
T (°C)	250		290		325	
$t^*(T)$ (h)	119.5		8.5		1.1	

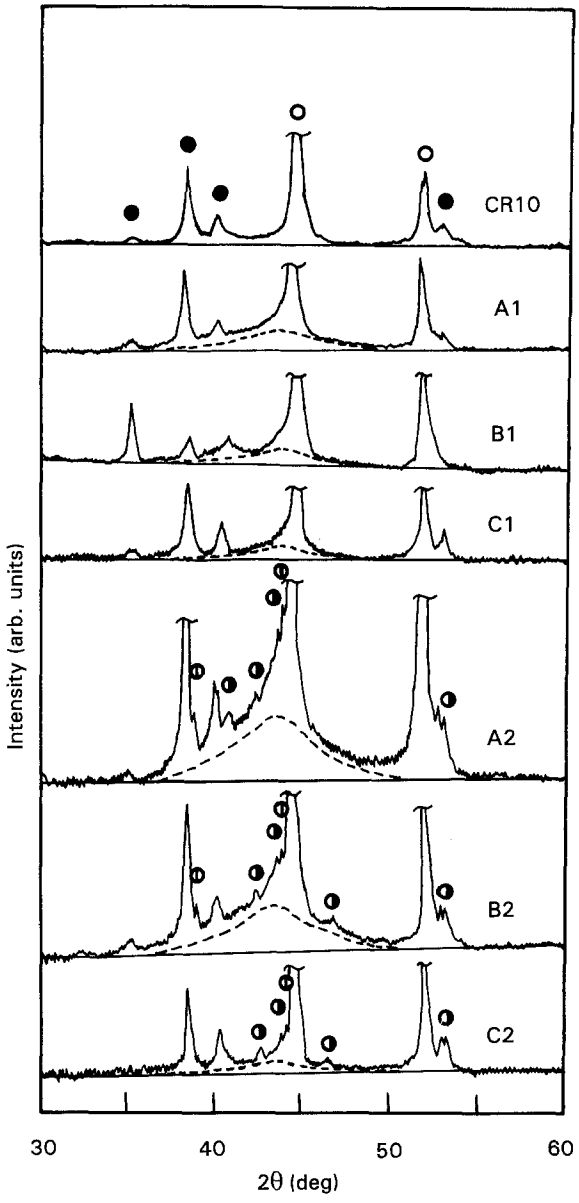

Figure 1 X-ray profiles for as-deformed multilayer (CR10) and the CR10 annealed at (A1) 250 °C for 100 h, (B1) 290 °C for 7 h, (C1) 325 °C for 0.9 h, (A2) 250 °C for 190 h, (B2) 290 °C for 10 h, and (C2) 325 °C for 1.3 h, respectively. (– – –) The assumed broad peaks resulting from amorphous phases. (○) Ni, (●) Ti, (⦶) NiTi, (◑) Ni_3Ti.

TABLE II Saturation magnetizations, M_s, amorphous interlayer thickness, W_e, calculated from M_s, and amorphous interlayer thickness W_c calculated according to the transient nucleation model.

	CR10	A1	B1	C1
M_s(e.m.u. g^{-1})	33.8	23.8	27.9	29.0
W_e (nm)	0	35.2	25.1	22.3
W_c (nm)	0	52.7	40.0	32.1
W_e/W_c	–	0.67	0.63	0.69

broad intensity profile, as shown in Fig. 1. The position centred at $2\theta \simeq 43.5°$ and the width of the assumed amorphous intensity profile are in good agreement with literature values for amorphous $Ni_{63}Ti_{37}$ glass [24, 25]. Upon prolonged annealing, all of the X-rays show peaks of intermetallic compounds, Ni_3Ti and NiTi, in the annealed CR10 samples, A2, B2, and C2. The intermetallic compounds occur after 1.3 h annealing at 325 °C, while they do not appear after 100 h annealing at 250 °C. This indicates that the isothermal annealing temperature and annealing time are very important to the SSAR in the Ni/Ti multilayers.

The saturation magnetizations, M_s, of the as-deformed and annealed multilayers are shown in Table II. The amorphous Ni–Ti alloy and elemental titanium are paramagnetic, while elemental nickel is ferromagnetic. Therefore, the decrease in M_s reveals the amorphization of elemental nickel and titanium.

The microstructures and the corresponding selected-area diffraction pattern for the annealed samples, A1 and C1, are shown in Fig. 2. A halo-like diffraction pattern, which is indicative of amorphous phase, can be clearly seen in the two samples. This directly supports the XRD and magnetic measurement experiments. The composition of the amorphous phase, as determined by EDAX detector, is $Ni_{63}Ti_{37}$ for sample A1 and $Ni_{69}Ti_{31}$ for sample C1, respectively. The compositions are in good agreement with the XRD analysis, which shows the existence of an amorphous alloy of composition near $Ni_{63}Ti_{37}$ [24, 25].

4. Discussion

For the SSAR in a metal multilayer system, a planar growth of the growing phase is expected for a heterogeneous reaction of a binary system [26], i.e. starting with an unreacted multilayer package, the formation of an amorphous phase is at every metal A/B interface after annealing. The amorphous alloy forms as a planar, very uniform layer between the crystalline reactants, as shown by the CS–TEM pictures [26]. In our Ni/Ti multilayered composites, transmission electron micrographs of samples A1 and C1 shown in Fig. 2 clearly indicate the existence of the amorphous regions after annealing. Because the slices used for the TEM observation are cut along the direction of the surface of the rolled product, that is, the direction parallel to the Ni/Ti interfaces, the completely amorphous region growing as a planar layer perpendicular to the Ni/Ti interface can be easily found by the TEM technique. However, it should be noted that the greater part of the annealed multilayer is still

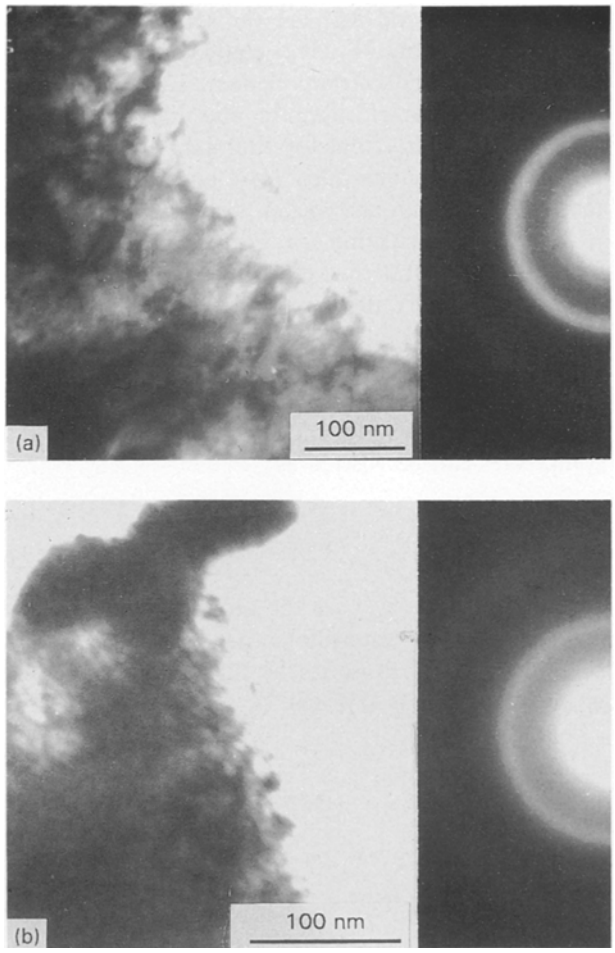

Figure 2 Transmission electron micrographs and the corresponding selected-area electron diffraction patterns for samples (a) A1 and (b) C1 described in Fig. 1.

crystalline because of the too thick elemental layers, as shown in Fig. 1.

It has been observed that as amorphous layers thicken by interdiffusion in A–B multilayers, a critical thickness, W_c, is reached beyond which intermetallic phases nucleate and grow to the detriment of further amorphization [26]. The critical thickness has been explained by various theoretical ideas [27–29]. Highmore *et al.* [28] suggested that for temperatures far below the equilibrium liquidus, and for nucleation at a moving interface, transient nucleation kinetics might predominate. A transition nucleation model [30] is used to represent information about the transition from growing amorphous alloy to growing a crystalline intermetallic on two kinds of map: one of layer thickness against temperature, the other of temperature against annealing time. The transient nucleation model was used in the present work.

The amorphous layer thickness, W_e, in the annealed Ni/Ti multilayers A1, B1, and C1, can be obtained from the volume fraction, X_{am}, of amorphous phase:

$$W_e = X_{am} \times (\mathrm{ASLT}) \quad (1)$$

where ASLT is the average single-layer thickness of the as-deformed Ni/Ti multilayer. X_{am} can be written as

$$X_{am} = (M_s^0 - M_s^1)[d_{Ti} + d_{Ni}X_{Ti}M_{Ti}/(X_{Ni}M_{Ni})]/ \times [M_s^0(d_{Ti} - d_{Ni}) + M_s^{Ni}d_{Ni}] \quad (2)$$

where M_s^0, M_s^1 and M_s^{Ni} are the saturation magnetizations of starting $Ni_{65}Ti_{35}$ coated powders, of annealed CR10, and of pure elemental nickel; d_{Ti} and d_{Ni} are densities of titanium and nickel; X_{Ti} and X_{Ni} are atom fractions of titanium and nickel in $Ni_{63}Ti_{37}$ amorphous alloy; M_{Ti} and M_{Ni} are mole masses of titanium and nickel, respectively.

A detailed derivation for Equation 2 is given as follows. Elemental nickel is ferromagnetic while amorphous Ni–Ti alloys and elemental titanium are not. Ignoring the change of atom volume after mixing and that of form factor of the magnetic phase after heating and reaction, the volume fraction of amorphous phase, X_{am}, for the annealed Ni/Ti multilayered composites can be written as

$$X_{am} = (W_{Ni}^{Am}/d_{Ni} + W_{Ti}^{Am}/d_{Ti})/(W_{Ni}/d_{Ni} + W_{Ti}/d_{Ti}) \quad (3)$$

where W_{Ni}^{Am} and W_{Ti}^{Am} are the atom masses of nickel and titanium in amorphous Ni–Ti alloy, whereas W_{Ni} and W_{Ti} are those in the starting Ni/Ti coated powders. W_{Ni}^{Am} and W_{Ti}^{Am} can be calculated from

$$W_{Ni}^{Am} = (M_s^0 - M_s^1)/M_s^{Ni} \quad (4)$$

$$W_{Ti}^{Am} = (W_{Ni}^{Am} X_{Ti} M_{Ti})/(X_{Ni} M_{Ni}) \quad (5)$$

while W_{Ni} and W_{Ti} can be written as

$$W_{Ni} = M_s^0/M_s^{Ni} \quad (6)$$

$$W_{Ti} = 1 - W_{Ni} \quad (7)$$

thus, Equation 2 can be easily derived according to Equations 3–7.

The derivation of the volume fraction of amorphous alloy from Equation 2 is affected virtually by the layered structure of nickel and its grain size. For example, the saturation magnetization of starting $Ni_{65}Ti_{35}$ composite powders and of the product after ten rolling passes is 38.0 and 33.8 e.m.u. g^{-1}, respectively. The decrease of saturation magnetization for the rolled product may be attributed mainly to the nanocrystalline Ni/Ti multilayered structure, which was verified by the TEM observation [22] and elucidated in the published report [31]. The decrease of saturation magnetization may result in an overestimate of the volume fraction of an amorphous alloy. This effect, however, may be diminished partially because of the growth of grains after annealing.

According to Equations 1 and 2, W_e is obtained and shown in Table II. W_e can be thought to be the critical amorphous-layer thickness corresponding to various isothermal annealing temperatures, because further annealing of A1, B1 and C1 samples will produce intermetallic compounds of nickel and titanium, as revealed by the XRD results.

According to the transient nucleation model, the critical thickness, $W_c(T)$, of amorphous alloy can also be determined by the expression [30]

$$W_c(T) = -\frac{f\tilde{D}}{3x(1-x)}\left(\frac{\pi}{6v}\right)^{1/3}\frac{kT\lambda^2}{D\Delta g} \quad (8)$$

where f is the fractional composition range over which the amorphous phase exists, $\tilde{D}$ is the effective interdiffusion coefficient in the amorphous layer, x is the average composition of the amorphous layer, v is the volume of one molecule of hexagonal Ni_3Ti, k is Boltzmann's constant, T is the temperature, λ is the diffusional jump distance, D is the effective diffusivity of molecules at the surfaces of a cluster, and Δg is the driving force for addition of one molecule to a cluster of Ni_3Ti.

The critical annealing times, $t^*(T)$, necessary for nucleation of the hexagonal Ni_3Ti phase during isothermal reaction at different temperatures can be calculated from the expression [30]

$$t^*(T) = \frac{f\tilde{D}}{18x(1-x)}\left(\frac{\pi}{6v}\right)^{2/3}\left(\frac{kT\lambda^2}{D\Delta g}\right)^2 \quad (9)$$

The diffusion coefficients, $\tilde{D}$ and D, were assumed to have Arrhenius temperature dependencies

$$\tilde{D} = \tilde{D}_0 \exp[-E/(kT)] \quad (10)$$

$$D = D_0 \exp[-Q/(kT)] \quad (11)$$

The thickness, $W_c(T, t)$, of amorphous layer formed during isothermal annealing for annealing times shorter than $t^*(T)$ can be calculated from [30]

$$W_c(T, t) = \left\{\frac{2f\tilde{D}_0}{x(1-x)} t \exp[-E/(kT)]\right\}^{1/2} \quad (12)$$

where t is the isothermal annealing time.

The parameters in Equations 8–12 are determined as follows: $f = 0.44$ [30, 32], $x = 0.63$, $v = 4.65 \times 10^{-29}$ m^3, $\lambda = 2.91 \times 10^{-10}$ m [30, 33], $\Delta g = 2.9 \times 10^{-20}$ J mol^{-1} [30, 32], $\tilde{D}_0 = 1.6 \times 10^{-8}$ m^{2}s^{-1} [22, 30], $E = 1.34$ eV at^{-1} [22, 30], $D_0 = 8.6 \times 10^{-10}$ m^{2}s^{-1} [30, 33], $Q = 1.56$ eV at^{-1} [30, 33].

Accordingly, $t^*(T)$ calculated from Equation 9 is 11.2 h when $T = 290$ °C. In fact, the hexagonal Ni_3Ti phase may appear at some time ranging from 7–10 h when the isothermal annealing temperature, T, is 290 °C, as revealed by the XRD profiles. Thus we take t^*(290 °C) to be 8.5 h for the corrections of D, because the parameter D is likely to be higher than the estimated D based on titanium [28]. $W_c(T)$ and $t^*(T)$, as calculated from Equations 8–11 with the corrected parameter D, are shown in Figs 3 and 4, respectively. Selected values of $t^*(T)$ theoretically calculated are also shown in Table I for comparison with the experimentally chosen annealing temperature and time. The relationship between the isothermal annealing time, t, is calculated according to Equation 12 and shown in Fig. 4 assuming a constant amorphous layer thickness $W_c(T, t)$.

It can be seen from Fig. 3 that the critical thickness, $W_c(T)$, of amorphous layer formed during isothermal annealing increases drastically with decreasing annealing temperature, T. For example, W_c(300 °C) is calculated to be 41.3 nm, while W_c(200 °C) is 87.0 nm. In other words, if bulk amorphization is wanted in the present Ni/Ti multilayer which has an ASLT of about 90 nm, the isothermal annealing temperature, T, should not be higher than 200 °C. In contrast, Schultz has isothermally annealed a Ni/Ti multilayer with an ASLT of 150 nm at 325 °C [11], which corresponds to a W_c(325 °C) of 35.8 nm. Thus the bulk amorphization

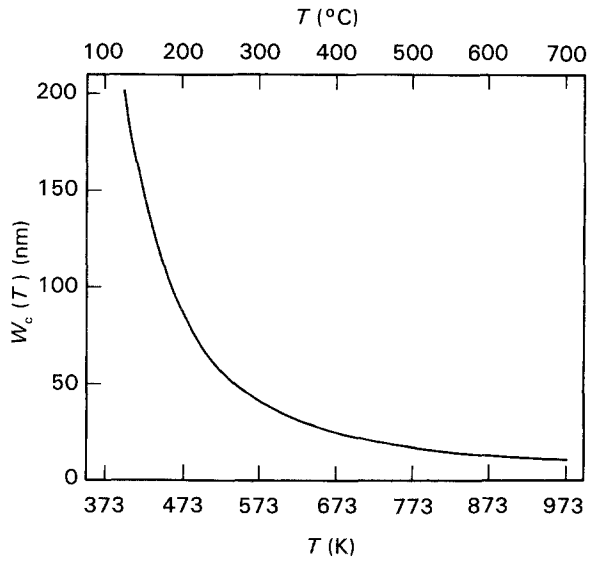

Figure 3 Critical amorphous layer thickness, $W_c(T)$, plotted against isothermal annealing temperature, T, for the Ni/Ti multilayers.

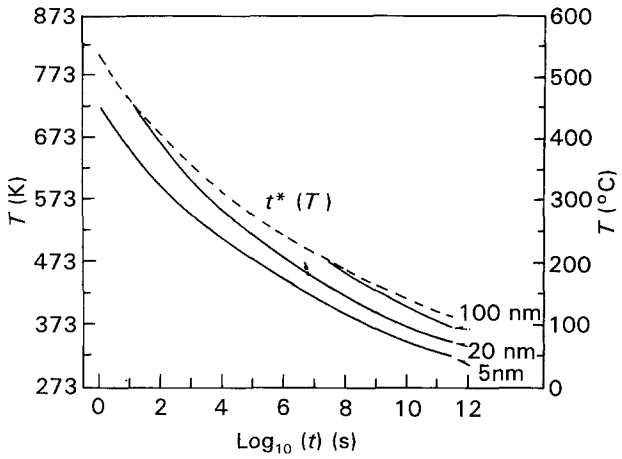

Figure 4 (——) The relationship between isothermal annealing temperature, T, and isothermal annealing time, t, calculated assuming a constant amorphous layer thickness, $W_c(T, t)$, for the Ni/Ti multilayer. (– – –) The calculated critical annealing time, $t^*(T)$, beyond which the transition from growing amorphous alloy to growing intermetallic compounds will occur.

has not been obtained with the Ni/Ti multilayer [11]. However, the decrease of T will lead to the drastic increase of isothermal annealing time, t, for a given amorphous layer thickness $W_c(T, t)$, as shown in Fig. 4. For example, to obtain bulk amorphization in the Ni/Ti multilayers with ASLT 90 and 150 nm, T should not be higher than 200 and 150 °C, the corresponding t should be 2.26×10^7 s (= 262 days) and 3.12×10^9 s (= 99 years), respectively. Nevertheless, T and t should be 270 °C and 1.08×10^5 s (= 30 h), respectively, for a Ni/Ti multilayer with an ASLT of 50 nm. This indicates that a reasonable ASLT is very important in the bulk amorphization in the Ni/Ti multilayer.

Fig. 1 and Tables I and II clearly show that the calculations for $t^*(T)$ and $W_c(T)$ are rather reasonable when compared with the experimentally obtained data of $t^*(T)$ and of W_c derived from the saturation magnetizations. Moreover, the thickness of the grown amorphous layer in Ni/Ti bilayer thin films, as determined by CS-TEM observation, was about 20 nm after annealing at 300 °C for 2 h [34], whereas Equation 12 gives a $W_c = 27.2$ nm. The ratio of the experimetally observed thickness to the theoretically calculated one is 0.74, indicating that the calculations from Equation 12, based on the hypothesis that for at least part of the SSAR the amorphous alloy grows by a diffusion-controlled layer process and that the growing amorphous inter layer exhibits a linear concentration profile with constant interfacial compositions [35], seems rather reasonable.

It has been reported that the various approximations in Equations 8, 9 and 12 may result in an overestimate of volume fraction of an amorphous phase, as elucidated elsewhere [28]. This is also true in our report, as shown in Table II. The oxygen absorbed at the Ni/Ti interfaces may react with titanium and release a large amount of heat, thus changing the reaction kinetics of the SSAR in the multilayered composites. This effect may result in an overestimate of the interdiffusion coefficient, $\tilde{D}$[36]. Additionally, it has been reported [37, 38] that during the SSAR, crystalline materials transform into an amorphous alloy not only at the Ni/Ti interfaces, on which a diffusion-controlled layer growth mechanism of the SSAR is based, but also along the grain boundaries. Further study is needed to classify these effects.

5. Conclusion

We have shown that single-phase amorphous Ni–Ti alloy can be synthesized by isothermal annealing of a mechanically deformed Ni/Ti multilayer. It has been found that as amorphous layers thicken by annealing-induced interdiffusion reaction in Ni/Ti multilayer, a critical amorphous layer thickness and a corresponding critical annealing time may be reached, beyond which intermetallic compounds of nickel and titanium nucleate and grow. The bulk amorphization can be obtained in the Ni/Ti multilayer with an ASLT thinner than the thickness of the critical amorphous layer during isothermal annealing. The dependence of the growth of the amorphous phase on the thermodynamic and kinetic parameters, on the isothermal annealing temperature, and on the isothermal annealing time in mechanically deformed Ni/Ti multilayer, has been quantitatively studied by a transient nucleation model. The theoretical calculations are in good agreement with the experiment results. It is believed that the quantitative studies may provide a direction for the bulk amorphization in the Ni/Ti or other metal–metal multilayer.

Acknowledgements

Valuable discussions with Dr R. J. Highmore are gratefully acknowledged. This work was supported by the National Natural Science Foundation of China.

References

1. R. B. SCHWARZ and W. L. JOHNSON, *Phys. Rev. Lett.* **51** (1983) 415.

2. B. M. CLEMENS, W. L. JOHNSON and R. B. SCHWARZ, *J. Non-Cryst. Solids* **61, 62** (1984) 817.
3. M. ATZMON, J. D. VERHOEVEN, E. D. GIBSON and W. L. JOHNSON, *Appl. Phys. Lett.* **45** (1984) 1052.
4. H. SCHRODER, K. SAMWER and U. KOSTER, *Phys. Rev. Lett.* **54** (1985) 197.
5. L. SCHULTZ, in "Proceedings of the MRS Europe Meeting on Amorphous Metal and Non-Equilibrium Processing", Strasbourg, 1984, edited by M. V. Allmen (Les Editions de Physique, Les Ulis, 1984) p. 135.
6. M. ATZMON, K. M. UNRUH and W. L. JOHNSON, *J. Appl. Phys.* **58** (1985) 3865.
7. L. SCHULTZ, in "Proceedings of the 5th International Conference on Rapidly Quenched Metals", Wurzburg, 1984, edited by S. Steeb and H. Warlimont (North-Holland, Amsterdam, 1985) p. 1585.
8. M. ATZMON, J. VERHOEVEN, E. D. GIBSON and W. L. JOHNSON, *ibid.*, p. 1561.
9. B. M. CLEMENS, *Phys. Rev.* **33B** (1986) 7615.
10. H. U. KREBS and K. SAMWER, *Europhys. Lett.* **2** (1986) 141.
11. L. SCHULTZ, "Amorphous and Liquid Metals", Proceedings NATO, Advanced Study Institute Series (NASA, Passo della Mendola, 1985) (1987) p. 508.
Jacucci (1987) p. 508.
12. *Idem, Z. Phys. Chem.* **157** (1988) 257.
13. F. BORDEAUX, A. R. YAVARI and P. DESER, *Mater. Sci. Eng.* **97** (1988) 129.
14. G. C. WONG, W. L. JOHNSON, E. J. COTTS, *J. Mater. Res.* **5** (1990) 488.
15. W. L. JOHNSON, *Prog. Mater. Sci.* **30** (1986) 80.
16. E. J. COTTS, W. J. MENG and W. L. JOHNSON, *Phys. Rev. Lett.* **57** (1986) 2295.
17. R. J. HIGHMORE, J. E. EVETTS, A. L. GREER and R. E. SOMEKH, *Appl. Phys. Lett.* **50** (1987) 566.
18. W. J. MENG, B. FULTZ, E. MA and W. L. JOHNSON, *ibid.* **51** (1987) 661.
19. B. M. CLEMENS, *J. Appl. Phys.* **61** (1987) 4525.
20. B. M. CLEMENS and J. G. GAY, *Phys. Rev.* **35B** (1987) 9337.
21. K. SAMWER, *Phys. Rep.* **161** (1988) 1.
22. T. D. SHEN, M. X. QUAN and J. T. WANG, *J. Mater. Sci.* **28** (1993) 394.
23. K. Y. WANG, T. D. SHEN, M. X. QUAN and J. T. WANG, *J. Mater. Sci. Lett.* **11** (1992) 129.
24. K. H. BUSCHOW, *J. Phys.* **F13** (1983) 563.
25. J. F. JONGSTE, M. A. HOLLANDERS, B. J. THIJSSE and E. J. MITTEMEIJER, *Mater. Sci. Eng.* **97** (1988) 101.
26. S. B. NEWCOMB and K. N. TU, *Appl. Phys. Lett.* **48** (1986) 1436.
27. W. J. MENG, C. W. NIEH and W. L. JOHNSON, *J. Appl. Phys.* **51** (1987) 1963.
28. R. J. HIGHMORE, A. L. GREER, J. A. LEAKE and J. E. EVETTS, *Mater. Lett.* **6** (1988) 401.
29. U. GÖSELE and K. N. TU, *J. Appl. Phys.* **66** (1989) 2619.
30. R. J. HIGHMORE, *Philos. Mag.* **62B** (1990) 455.
31. H. GLEITER, *Prog. Mater. Sci.* **33** (1989) 223.
32. R. B. SCHWARZ, R. R. PETRCH and C. K. SAW, *J. Non-Cryst. Solids* **76** (1985) 281.
33. C. J. SMITHELS, "Metals Reference Book", 5th Edn (Butterworth, London, 1976) p. 860.
34. M. KITHDA, N. SHIMIZU and T. SHIMOTSU, *J. Mater. Sci. Lett.* **18** (1989) 1393.
35. U. GÖSELE and K. N. TU, *J. Appl. Phys.* **53** (1982) 3252.
36. T. D. SHEN, J. T. WANG, M. X. QUAN and W. D. WEI, *J. Non-Cryst. Solids* **150** (1992) 464.
37. M. A. HOLLANDERS and B. J. THIJSSE, *ibid.* **117/118** (1990) 696.
38. M. A. HOLLANDERS, B. J. THIJSSE and E. J. MITTEMEIJER, *Phys. Rev. B* **42** (1990) 5481.

Received 18 March
and accepted 19 October 1993